

This article was downloaded by: [Siauliai University Library]

On: 17 February 2013, At: 06:47

Publisher: Taylor & Francis

Informa Ltd Registered in England and Wales Registered Number: 1072954 Registered office: Mortimer House, 37-41 Mortimer Street, London W1T 3JH, UK



Advanced Composite Materials

Publication details, including instructions for authors and subscription information:

<http://www.tandfonline.com/loi/tacm20>

Monitoring of dynamical processes in PAAm-MWNTs composites by fluorescence method

Gülşen Akın Evingür^a & Önder Pekcan^b

^a Piri Reis University, Tuzla, İstanbul, 34940, Turkey

^b Kadir Has University, Cibali, İstanbul, 34083, Turkey

Version of record first published: 28 Jun 2012.

To cite this article: Gülşen Akın Evingür & Önder Pekcan (2012): Monitoring of dynamical processes in PAAm-MWNTs composites by fluorescence method, *Advanced Composite Materials*, 21:2, 193-208

To link to this article: <http://dx.doi.org/10.1080/09243046.2012.690299>

PLEASE SCROLL DOWN FOR ARTICLE

Full terms and conditions of use: <http://www.tandfonline.com/page/terms-and-conditions>

This article may be used for research, teaching, and private study purposes. Any substantial or systematic reproduction, redistribution, reselling, loan, sub-licensing, systematic supply, or distribution in any form to anyone is expressly forbidden.

The publisher does not give any warranty express or implied or make any representation that the contents will be complete or accurate or up to date. The accuracy of any instructions, formulae, and drug doses should be independently verified with primary sources. The publisher shall not be liable for any loss, actions, claims, proceedings, demand, or costs or damages whatsoever or howsoever caused arising directly or indirectly in connection with or arising out of the use of this material.

Monitoring of dynamical processes in PAAm–MWNTs composites by fluorescence method

Gülşen Akın Evingür^a and Önder Pekcan^{b*}

^aPiri Reis University, Tuzla, İstanbul 34940, Turkey; ^bKadir Has University, Cibali, İstanbul 34083, Turkey

(Received 16 October 2011; accepted 30 April 2012)

Polyacrylamide (PAAm)–multi walled carbon nanotube (MWNT) composites were prepared by free radical cross-linking copolymerization in water. Ammonium persulfate and *N,N'*-methylenebis (acrylamide) (BIS) were used as a free radical initiator and a crosslinker, respectively. The drying and swelling processes of disc shaped PAAm–MWNT composites were monitored by the steady-state fluorescence technique at various temperatures. Disc shaped composite gels were prepared with pyranine (*P*) doped as a fluorescence probe. Scattered, I_{sc} , and emission light, I_{em} , intensities were monitored during drying and swelling of these gels. Since the decrease and increase in I_{sc} corresponds to the decrease and increase in turbidity of the drying and swelling hydrogel, respectively, the corrected fluorescence intensity, I was introduced to analyse the drying and swelling processes. The Stern-Volmer equation combined with moving boundary and Li–Tanaka models were used to explain the behavior of I during drying and swelling processes, respectively. Results indicated that the desorption coefficient, D_d decreased by increasing MWNT content, until 1 weight percentage of MWNT is reached and then increased above 1 wt% MWNT for a given temperature during drying. However, cooperative diffusion coefficient, D_s behaved opposite to D_d during swelling at a given temperature. Supporting gravimetric and volumetric experiments were also carried out during drying and swelling of PAAm–MWNT composite gels.

Keywords: multi walled carbon nanotubes (MWNT); acrylamide; composite; fluorescence; temperature; drying; swelling

1. Introduction

Carbon nanotubes (CNTs) are closed graphene sheets with a cylindrical shape with end caps. They have diameters ranging from about a nanometer to tens of nanometres and lengths up to centimetres. Composites of CNTs in polymeric materials have attracted considerable attention in the research and industrial communities due to their unique mechanical and electrical properties. CNT polymer nanocomposites possess high stiffness, high strength and good electrical conductivity at relatively low concentrations of CNT filler [1]. Swelling and mechanical behaviour of a novel gelatine–CNT hybrid hydrogel was performed by a scanning electron microscope. This study suggested that the hybrid gelatine hydrogel with CNTs could be used in biomedical field [2]. Synthesis of the same hybrid hydrogel was prepared by physical mixing method. The results indicated that the novel hybrid hydrogel produced high mechanical property and used in drug delivery of gelatine–MWNTs gel [3]. Mechanical reinforcement of

*Corresponding author. Email: pekcan@khas.edu.tr

CNT polymer composites was reviewed [4]. Swelling and mechanical behaviours of CNTs/poly(vinyl alcohol) hybrid hydrogels were investigated as the basis of the application of CNTs in the field of biomaterials [5]. Modulation of single-walled CNTs photoluminescence by hydrogel swelling demonstrated that the shift of nanotubes photoluminescence occurred in a hydrogel matrix. As the hydrogel cross-linking density and hydration state is changed, the nanotubes experience lattice deformations and a shift in photoluminescence emission maxima was observed [6]. Poly(N-isopropylacrylamide) (PNIPAAm) containing single-walled carbons and single-walled nanohorns showed phase transitions [7]. Preparation and characterization of PAAm/MWNTs nanohybrid hydrogels with microporous structures was presented by mechanical, pH and temperature sensitive response and swelling kinetics [8]. The addition of nanotubes produced interesting properties, including tailor ability of temperature responsive swelling and mechanical strength of the PNIPAAm–MWNT composites. The mechanical properties of the nanocomposites were studied over a range of temperatures to characterize the effect of nanotubes addition [9]. Mechanically fragile Poly (N,N-diethylacrylamide) (PDEA)-co-polyacrylic (PAA) composite hydrogels were studied with respect to temperature, pH, strength and MWNT rates. The results showed that the synthesized nanocomposites would be useful in medicine and pharmaceuticals [10]. Rheological, thermal and damping properties were presented in a review study including dispersion and functionalizations of CNTs for polymer-based nanocomposites [11].

Low and high water sorption properties of hydrogels may be important for the use of sorbents in many applications of biomaterials and separation operations in biotechnology, drug delivery systems, processing of agricultural products, sensors and actuators [12]. Several experimental techniques have been employed to study the kinetics of drying of chemical and physical gels e.g. neutron scattering, quasielastic light scattering [13], macroscopic experiments [14] and *in situ* interferometric measurements [15]. The steady-state fluorescence (SSF) technique was used to study the drying of PAAm gels with various κ -car contents [16] and with temperatures [17]. Recently, the fast transient fluorescence technique was used in our laboratory to study gel drying processes [18,19].

The photon transmission technique was used to study the swelling of PAAm gels with various crosslinker contents [20,21]. The decrease in transmitted light intensity, I_{tr} , was modelled using the Li–Tanaka equation from which cooperative diffusion coefficients, D , were determined for various BIS content PAAm gels; the decrease in I_{tr} was attributed to lattice heterogeneities, which might have originated between microgels and holes in the swelling gel. It was observed that cooperative diffusion coefficients decreased as the crosslinker content was increased. We reported the PAAm hydrogel swelling for various temperatures and crosslinker contents by using SSF technique [22,23]. It was observed that cooperative diffusion coefficients increased and decreased as the swelling temperature and crosslinker content were increased, respectively. The SSF technique was also used to study the swelling properties of PAAm- κ -carrageenan composite gels prepared in various κ -carrageenan concentrations and temperatures, respectively. It has been reported that high κ -car content composites swell much faster due to having larger of D_s coefficients for all measurements compared to low κ -car content composites for a given temperature [17,24]. The results presented in this preliminary works suggest that the fluorescence method can be used to measure diffusion coefficients at a molecular level during swelling of hydrogel with MWNT.

Here, we firstly report the drying and swelling process of PAAm–MWNT composites by using the SSF technique. PAAm can be polymerized easily by free radical cross-linking copolymerization of AAm in the presence of *N,N'*-methylenebis (acrylamide) (BIS) as the crosslinker. By combining the Stern-Volmer equation with the moving boundary model desorption coefficients, D_d , were determined for PAAm–MWNT composites during drying.

The desorption coefficients, D_d , decreased by increasing MWNT content, until 1 wt% MWNT and then increase above 1 wt% MWNT for a given temperature during drying. The Li–Tanaka equation was used to determine the swelling time constants, τ_s , decreased by increasing MWNT content, until 1 wt% MWNT is reached and then increase above 1 wt% MWNT and cooperative diffusion coefficients, D_s , behaved in a reverse manner to the drying behaviour during swelling at a given temperature. Supporting gravimetric and volumetric experiments were also carried out where similar behaviour was observed for the measured parameters for PAAm–MWNT composites during drying and swelling processes, respectively.

2. Theoretical considerations

2.1. Stern–Volmer kinetics

This model is based on the variations of quantum yields of photo physical processes such as fluorescence, phosphoresce and photochemical reactions with the concentration of a given quencher. The Stern–Volmer type of quenching mechanism can be proposed for the fluorescence intensity in the sample under consideration. According to the Stern–Volmer law, fluorescence intensity can be written as [25],

$$\frac{I_0}{I} = 1 + k_q \tau_0 [Q] \quad (1)$$

Here, k_q is quenching rate constant, τ_0 is the lifetime of the fluorescence probe with no quenching has taken place, $[Q]$ is the quencher concentration and I_0 is the fluorescence intensity for zero quencher content.

For low quenching efficiency, ($\tau_0 k_q [Q] \ll 1$), Equation (1) becomes

$$I \approx I_0 (I - \tau_0 k_q [Q]) \quad (2)$$

If one integrates Equation (2) over the differential volume (dv) of the sample from the initial a_0 to final a_∞ thickness, then reorganization of the relation produces the following useful equation.

$$W = \int_{a_0}^{a_\infty} [W] dv \quad (3)$$

In our case, the amount of water diffusion, W is calculated over differential volume by replacing Q with W as

$$W = \left(1 - \frac{I}{I_0}\right) \frac{v}{k_q \tau_0} \quad (4)$$

Here it is assumed that water molecules are the only quencher for the excited pyranine molecules in our system. Where v is the volume at the equilibrium swelling state, which can be measured experimentally, k_q was obtained from separate measurements by using Equation (1) where the infinity equilibrium value of water diffusion, W , was used for each sample. Since τ_0 is already known, then the measured values of I , W and V at the equilibrium swelling condition can be used to calculate k_q for each swelling experiment separately.

2.2. Moving boundary model

The moving interface can be marked by a discontinuous change in concentration as in the absorption by a liquid of a single component from a mixture of gases or by a discontinuity in the gradient of concentration as in the progressive freezing of a liquid [26]. When the diffusion coefficient is discontinuous at a concentration c i.e. the diffusion coefficient is zero below c and constant and finite above c then the total amount, M_t , of diffusing substance desorbed from the unit area of a plane sheet of thickness a at time t is given by the following relation

$$\frac{M_t}{M_f} = 2 \left[\frac{D_d}{\pi a^2} \right]^{1/2} t^{1/2} \quad (5)$$

where D_d is a diffusion coefficient at concentration c_1 . Here $M_f = ac_1$ is the equilibrium value of M_t . If one assumes that the diffusion coefficient of polymer segments in the gel is negligible compared to the desorption coefficient, D_d , of water, then Equation (5) can be written as follows:

$$\frac{W}{W_f} = 2 \left[\frac{D_d}{\pi a^2} \right]^{1/2} t^{1/2} \quad (6)$$

Here it is assumed that M_t is proportional to the amount of water molecules released, W , at time, t .

2.3. Li–Tanaka model

The kinetics of the swelling of a gel is comprehensively described by the behaviour of the displacement vector, \vec{u} as a function of space and time. Li and Tanaka showed that the equation of motion is given by [27]

$$\frac{\partial \vec{u}}{\partial t} = D_s \nabla^2 \vec{u} + \frac{K + \mu/3}{f} \vec{\nabla} \times (\vec{\nabla} \times \vec{u}) \quad (7)$$

where $D_s = (K + 4\mu/3)/f$ is the cooperative diffusion coefficient. f is the friction coefficient and μ is the shear modulus. Here, t denotes the time and K is the bulk modulus [27]. Equation (7) can also be solved and written in terms of water uptakes W and W_f at time t and equilibrium [27], respectively, as follows:

$$1 - \frac{W}{W_f} = \sum_{n=1}^{\infty} B_n \exp(-t/\tau_n) \quad (8)$$

In the limit of large t , or if τ_1 is much larger than the rest of τ_n , all higher terms $n \geq 2$ in Equation (8) can be omitted and the swelling kinetics is given by the following relation

$$\frac{W}{W_f} = 1 - B_1 \exp(-t/\tau_1) \quad (9)$$

where B_1 is given by the following relation:

$$B_1 = \frac{2(3 - 4R)}{\alpha_1^2 - (4R - 1)(3 - 4R)} \quad (10)$$

It should be noted from Equation (10) that $\sum B_n = 1$ therefore, B_1 should be less than 1. B_1 is related to the ratio, R , of the shear modulus, μ and longitudinal osmotic modulus, $M = (K + 4\mu/3)$. Once the value of B_1 is obtained, one can determine the value of $R = \mu/M$ [27]. τ_1 is related to the cooperative diffusion coefficient, D_s , at the surface of a gel disc by

$$D_s = \frac{3a_f^2}{\tau\alpha_f^2} \quad (11)$$

where α_1 is a function of R only [27] and a_f stands for the half thickness of the gel in the final equilibrium state. Hence, D_s can be calculated.

3. Experimental

We used MWNT which was analyzed by the Delta Nu Advantage 532 Raman Spectrometer with 100–3400 wave number spectral range (Cheap Tubes Inc., USA) with a length of 20–30 nm and a diameter of 10–30 μm . The purity of the MWNT was >95 wt%.

Initially, the solution is composed of MWNTs, PVP and water in the proportions of 10 parts MWNTs: 1–2 parts PVP: 2000 parts distilled water at room temperature. The required dispersion time is approximately 5 or 6 min with an interruption of 10 s, every 30 s at full or high amplitude by using ALEX ultrasonic equipment.

Composite gels were prepared by using 2 M AAm (Acrylamide, Merck) with various molar percentages (0.1–15 wt%) of MWNTs stock concentration at room temperature. AAm, the linear component; BIS (*N,N'*-methylenebisacrylamide, Merck), the crosslinker; APS (ammonium persulfate, Merck) the initiator and TEMED (tetramethylethylenediamine, Merck), the accelerator were dissolved in distilled water. The crosslinker, initiator and pyranine, P concentrations were kept constant at 0.013 M, 7×10^{-3} and 4×10^{-4} M, respectively, for all samples. The solution was stirred (200 rpm) for 15 min to achieve a homogenous solution. All samples were deoxygenated by bubbling nitrogen for 10 min, each pre-composite gel solution of 5 ml was poured into a cylindrical glass tube [28] and injector for drying and swelling experiments, respectively. Gelation, drying and swelling processes were performed by a Model LS-50 spectrometer of Perkin-Elmer, equipped with temperature controller. The beginning of the PAAm–MWNT gelation reaction, only the 512 nm peak exists, and then the intensity of the new (short-wavelength) peak around 380 nm starts to increase as the intensity of the 512 nm peak (long-wavelength) decreases during the course of gelation of PAAm–MWNT composite gels. The increase in 380 nm emission is due to a C–O ether bond formation between the hydroxyl oxygen of 3sPyOH and a terminal C-atom of the growing AAm chain [29]. As the polymerization proceeds, the maximum of the short-wavelength peak shifts to some higher wavelength, starting from 380 nm and ending at 427 nm [30]. The shift in the short-wavelength region between 380 and 427 nm is probably due to the complexation of SO_3^- groups with protonated amide groups, whether on the same polymer molecule or on the other polymer strands [29]. The reason for the shift in the isoemissive (isostilbic) point is the change in the internal morphology of the system. At the beginning of the polymerization the system is in the ‘sol’ state (all pyranine are free) and above a certain time it turns into the ‘gel’ state (most of the pyranine are bonded).

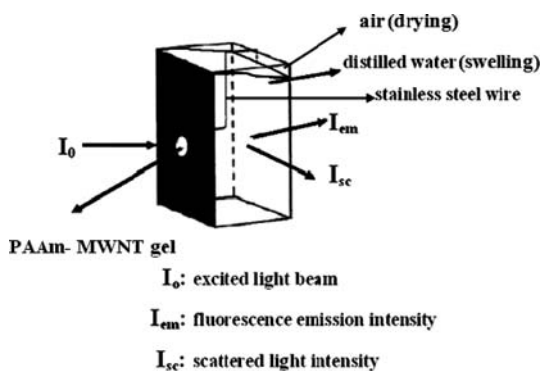


Figure 1. The position of PAAm–MWNT composite gels in the fluorescence cell during drying (in air) and swelling (in water). I_0 is excitation, I_{em} is emission and I_{sc} is scattered light intensities at 340 and 427 nm, respectively.

Before drying was started, composites were cut into discs with 10 mm in diameter and 4 mm in thickness from the injector. Disc shaped gel samples were placed on the wall of a 1 cm path length, square quartz cell filled with air and water for drying and swelling experiments, respectively. As soon as drying completed, swelling experiment was started. All measurements were made at 90° position and spectral bandwidths were kept at 5 nm. Pyranines in the PAAm–MWNT composite gels were excited at 340 nm during *in situ* experiments and emission intensities of the pyranine were monitored at 427 nm as a function of drying time. The position of the PAAm–MWNT composite gel which was behind the hole in the cell and fixed by stainless steel wire and the incoming light beam for the fluorescence measurements are shown in Figure 1 during drying and swelling of the composite gel in air and in distilled water, respectively. Here one side of the quartz cell is covered by black card-board with a circular hole which was used to define the incoming light beam and limits its size to the dimensions of the gel disc. The drying and swelling experiments of disc shape PAAm–MWNT composite gels prepared with various MWNT were performed in air and in water, respectively, at temperatures of 30, 40, 50 and 60 °C. At the same time, a gravimetric measurement was performed by measuring weight. The distance and thickness of the PAAm–MWNT composite gels were also measured to calculate the volume of the PAAm–MWNT composite gels from the formula for a cylinder's volume. The initial thickness is constant for the all samples.

4. Results and discussion

4.1. Drying

Figure 2 shows the emission spectra of pyranine from PAAm–MWNT composite gel during the drying process at 30 and 60 °C for 3 wt% MWNT content samples. It can be seen in Figure 2 that as the water release increases, fluorescence intensity, I_{em} , increases and the scattered light intensity, I_{sc} , decreases with increasing temperature. Since the decrease in I_{sc} corresponds to the decrease in turbidity of the drying gel, the corrected fluorescence intensity, I , is defined as I_{em}/I_{sc} to monitored exact behaviour of the fluorescence intensity i.e. as the drying time, t , is increased, the quenching of excited pyranines decrease due to an increase in the water release from the drying PAAm–MWNT composite gel. In order to quantify these results a collisional type of quenching mechanism may be proposed for the fluorescence

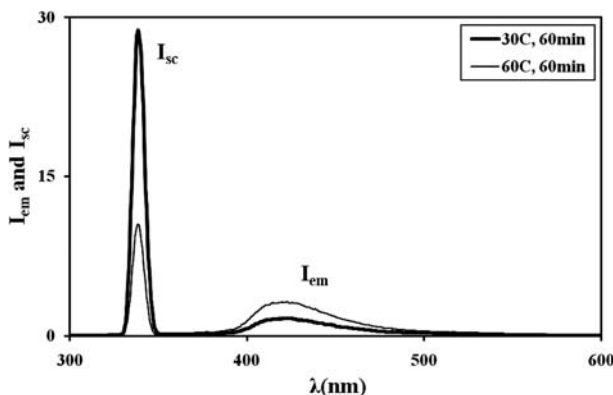


Figure 2. Emission spectra of pyranine from the hydrogel prepared with 3 wt% MWNT content samples during the drying process at 30 and 60 °C.

intensity, I from the gel samples during the drying process by using Equation (4). τ_0 is already known for pyranine so W can be calculated by using Equation (4) and the measured I values, in each drying step.

The plots of W vs. t at various MWNT content samples are presented in Figure 3(a) where the fit of the data to Equation (6) produced the desorption coefficient, D_{dl} , which are listed in Table 1. It is seen that D_{dl} values decreased until 1 wt% MWNT is reached and then increased to a plateau by presenting the different behaviours below and above the critical MWNT (1 wt%) content, (see Figure 4(a)) at which the conducting percolation cluster starts to appear [28]. At the critical point, D_{dl} presents a minimum due to the formation of percolation cluster from the MWNT.

On the other hand, by using gravimetric methods water desorption was also measured from the drying PAAm–MWNT composite gel prepared at various MWNT contents. The plots of the data are presented in Figure 3(b) at 30 and 60 °C for 10 wt% MWNT content gels. The fits of water release, W_w vs. $t^{1/2}$ to Equation (6) for the various MWNT content gel dried at various temperatures produce the desorption coefficients, D_{dw} , which are listed in Table 1, where it is observed that the desorption coefficient decreases up to 1 wt% MWNT content and then increases above 1 wt% MWNT for each temperature as was observed with fluorescence technique. The variations in volume, V of PAAm–MWNT composite gels during the drying process are also measured. The plots of the volume, V , vs. drying time for 10 wt% MWNT content PAAm–MWNT composite gel dried at 30 and 60 °C are presented in Figure 3(c). The data in Figure 3(c) is fitted to the following relation produced from Equation (6)

$$\frac{V}{V_f} = 2 \left(\frac{D_d}{\pi a^2} \right)^{1/2} t_d^{1/2} \quad (12)$$

Here it is assumed that the relation between W and V is linear. Then using Equation (12), the volumetric desorption coefficients, D_{dv} , were determined and listed in Table 1. Again, it is seen that D_{dv} values decreased from 0 to 1 wt% MWNT and then increased from 1 to 15 wt% MWNT at each temperature, similar to the behavior of D_{dw} . It has to be noted that, D_{dw} and D_{dv} coefficients are found to be much smaller than D_{dl} values at high MWNT content gels. These differences come from the measurement technique, i.e.

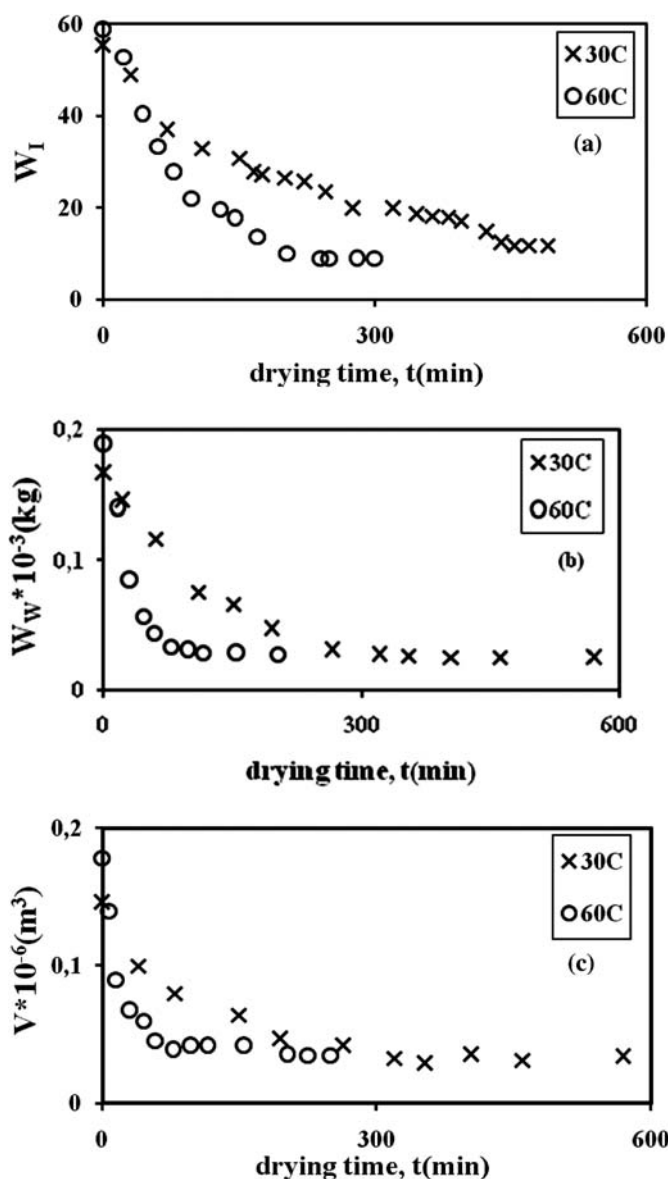


Figure 3. The plots of water release, W measured by (a) fluorescence, (b) gravimetric and (c) volumetric methods, vs. drying time, t , for PAAm-MWNT composite gels dried in air at 30 and 60 °C for 10 wt% MWNT content sample, respectively.

Fluorescence technique measures the D_{dI} values at a molecular level and however, D_{dW} and D_{dV} values present the bulk behaviour of the gel under consideration. Figure 4 summarized the desorption coefficients, D_d which were obtained from Equations (6) and (12) and measured by fluorescence, gravimetric and volumetric techniques for various MWNT content samples, respectively, where it was observed that the desorption coefficient decreased as the MWNT content is increased up to 1 wt% MWNT and then increased and reached to a plateau.

Table 1. Experimentally measured parameters of PAAm–MWNT composites for various MWNT content and temperature during drying process.

T (°C)	wt% MWNT	$D_{dl} \times 10^{-9}$ (m ² /s)	$D_{dw} \times 10^{-9}$ (m ² /s)	$D_{dv} \times 10^{-9}$ (m ² /s)
30	0.3	2.46	2.83	3.05
	0.6	2.30	2.40	2.90
	1	2.29	2.04	2.60
	3	2.30	2.60	2.99
	5	2.35	2.90	3.29
	10	2.46	3.05	3.44
	15	4	3.54	4
40	0.3	4.53	4.99	4.76
	0.6	3.17	3.15	2.76
	1	2.57	2.06	2.72
	3	6.23	2.76	3.29
	5	8.65	3.11	4.07
	10	9.88	4.39	4.14
	15	10.4	4.65	4.92
50	0.3	8.56	9.04	8.09
	0.6	6.08	8.39	6.64
	1	4.70	3.29	3.11
	3	8.39	3.41	4.18
	5	12.1	3.86	4.51
	10	14.3	5.38	5.38
	15	16.4	6.52	6.25
60	0.3	9.15	9.15	12.5
	0.6	7.37	8.72	11.5
	1	5.28	5.67	5.02
	3	10.2	6.36	6.16
	5	12.7	6.56	6.29
	10	14.2	7.47	6.52
	15	17.6	8.39	7.69

4.2. Swelling

Figure 5 shows the emission spectra of pyranine from PAAm–MWNT composite gel during the swelling processes at 30 and 60 °C for 3 wt% MWNT content samples, where the reverse behaviour of I_{em} and I_{sc} is observed in the PAAm–MWNT composite gel compared to the drying processes. As the swelling time, t , is increased, the quenching rate of excited pyranines increased due to water uptake. It should also be noted that quenching became more efficient for high molar percentage of MWNT content samples. In order to quantify these results, a collision type of quenching mechanism may be proposed for the fluorescence intensity, I , for the gel sample during the swelling process by using Equation (2). For pyranine, if τ_0 is known, then W can be calculated by using Equation (4) and the measured I values, at each step of the swelling [25]. Here, it is assumed that the k_q values do not vary during the swelling processes, i.e. the quenching process solely originates from the water molecules. Plots of water uptake, W , vs. swelling time are presented in Figure 6(a). The logarithmic form of the data in Figure 6(a) was fitted to the following relation produced from Equation (9)

$$\ln\left(1 - \frac{W}{W_f}\right) = \ln B_1 - \frac{t}{\tau_{sl}} \quad (13)$$

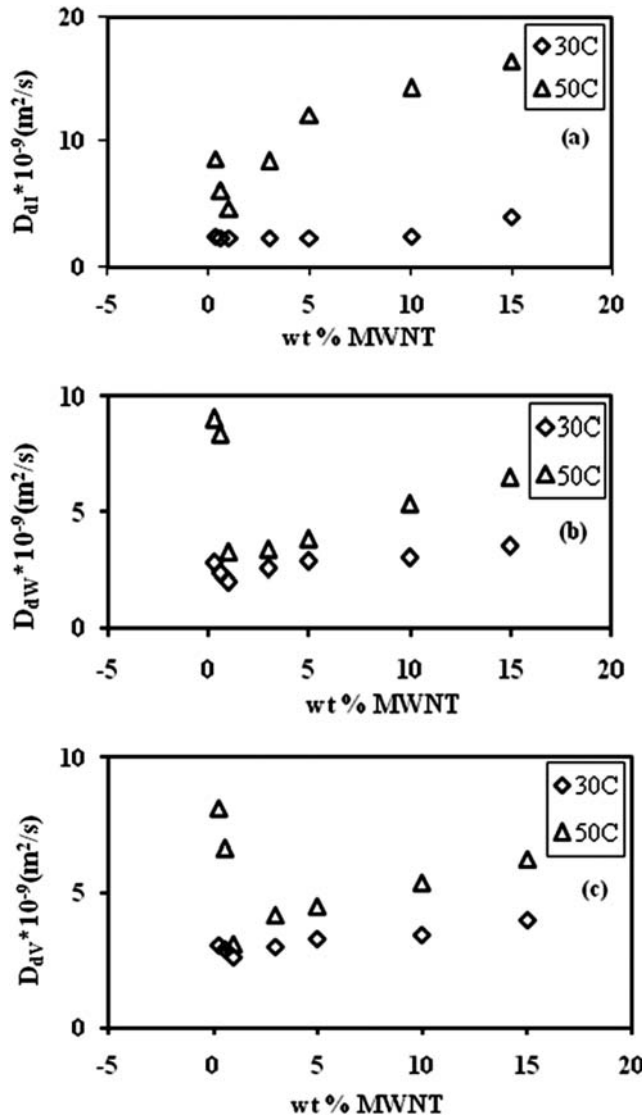


Figure 4. Desorption diffusion coefficients, D_d , vs. MWNT content measured by (a) fluorescence, (b) gravimetric and (c) volumetric techniques at 30 and 50 °C, respectively.

Here, τ_{sI} is the time constant and B_1 is related to the ratio of the shear modulus, μ and longitudinal osmotic modulus, M , by Equation (10). Using Equation (13) linear regression of the curves in Figure 6(a) provided us with B_1 and τ_{sI} values. Taking into account the dependence of B_1 on R , one obtains R values and from the α_1 – R dependence α_1 value was produced. The experimental determination of these values was based on the method described by Li and Tanaka [27]. Then, using Equation (11), cooperative diffusion coefficients D_s were determined for these disc-shaped gels and found to be around $10^{-9} \text{ m}^2/\text{s}$. Experimentally obtained τ_{sI} and D_{sI} values are summarized in Table 2. It should be noticed that D_{sI} values increased as the MWNT content is increased until 1 wt% MWNT is reached and then decreased by increasing molar percentage of MWNT content.

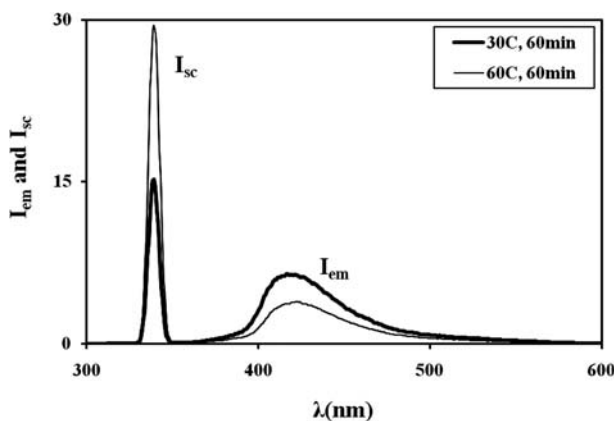


Figure 5. Emission spectra of pyranine from the hydrogel prepared with 3 wt% MWNT content samples during the swelling process at 30 and 60 °C.

The plots of the solvent uptake, W , vs. swelling time measured gravimetrically at 30 and 60 °C for 10 wt% MWNT content gel swollen in water are shown in Figure 6(b). These are typical solvent uptake curves obeying the Li–Tanaka equation, Equation (9). The logarithmic forms of the data in Figure 6(b) were fitted to the following relation produced from Equation (9),

$$\ln\left(1 - \frac{W}{W_f}\right) = \ln B_1 - \frac{t}{\tau_{sW}} \quad (14)$$

from which B_1 and the gravimetric time constant, τ_{sW} , were determined. Then, using Equation (11), gravimetric cooperative diffusion coefficients, D_{sW} , were determined and are listed in Table 2 with the τ_{sW} values. A similar behaviour in D_{sW} is observed as for D_{sI} as the MWNT contents were increased at the given temperatures.

The variations in the volume, V , of the PAAM–MWNT composites during the swelling process were also measured. The plots of the volume, V , vs. swelling time for PAAM–MWNT composites swollen in water are presented in Figure 6(c), which is again typical solvent uptake curves, obeying the Li–Tanaka equation, Equation (9). The logarithmic forms of the data in Figure 6(c) were fitted to the following relation as given in Equation (15) produced from Equation (9).

$$\ln\left(1 - \frac{V}{V_f}\right) = \ln B_1 - \frac{t}{\tau_{sV}} \quad (15)$$

from which B_1 and τ_{sV} were determined. Here it is assumed that the relation between W and V was linear. Then using Equation (11) the volumetric cooperative diffusion coefficients, D_{sV} were determined and are listed in Table 2. Again, it is seen that the D_{sV} values increased as the MWNT content is increased until 1 wt% MWNT and then decreased at each given temperature; similar to D_{sW} behavior. The D_{sW} and D_{sV} coefficients are found to be much smaller at high MWNT content gels. The produced D_s values from different techniques are summarized in Figure 7, where it is seen that all D_s values first increase up to 1 wt% MWNT content and reached its highest value at this critical point, where the percolation cluster from MWNT

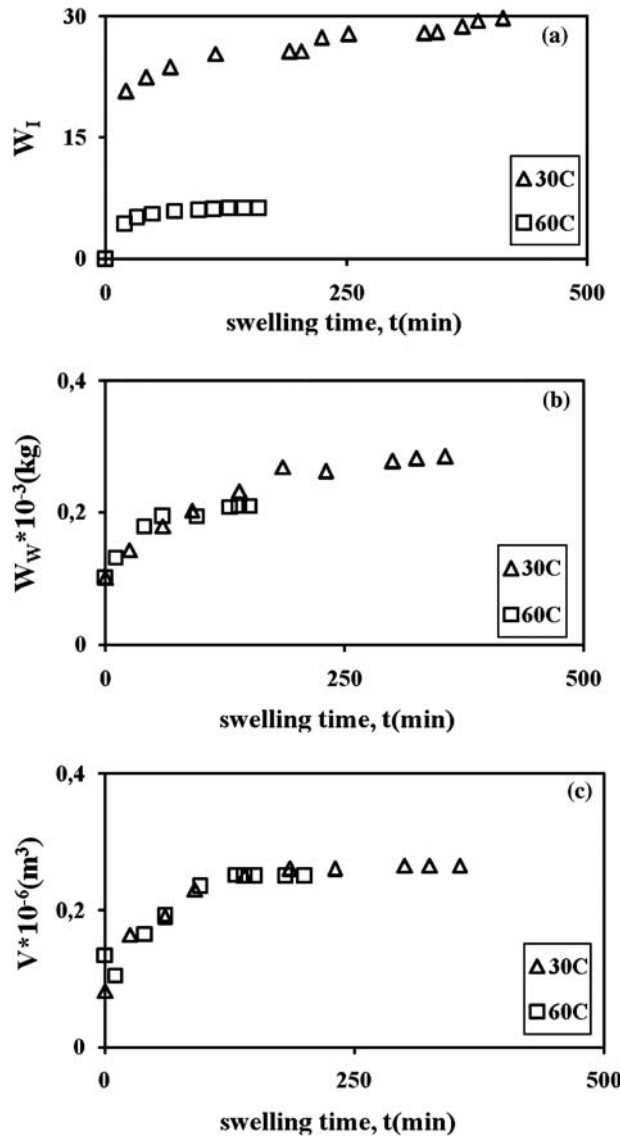


Figure 6. The plots of water uptake, W measured by (a) fluorescence, (b) gravimetric and (c) volumetric methods, vs. swelling time, t , for PAAm-MWNT composite gels swollen in water at 30 and 60 °C for 10 wt% MWNT content samples, respectively.

starts to form. The percolation cluster formed from CNTs helps water molecules flow faster in their channels and causes the composite gel swell faster presenting large D_s values for all samples under consideration. However above the critical point (1 wt% MWNT) composite gel is quite stiff due to the formation of infinite network from MWNT. The formation of inelastic composite gel above the critical point then lowers the D_s values to the smaller numbers.

The above picture can also explain the behaviour of desorption coefficient, D_d , in Figure 4. Since composite gel highly swollen at the critical point (1 wt% MWNT), then it takes longer time to dry, resulting lowest D_d values at this point. Above 1 wt% MWNT content, since

Table 2. Experimentally measured parameters of PAAm-MWNT composites for various temperatures and MWNT content during swelling process.

T (°C)	wt% MWNT	τ_{sl} (min)	$D_{sl} \times 10^{-9}$ (m ² /s)	τ_{sw} (min)	$D_{sw} \times 10^{-9}$ (m ² /s)	τ_{sv} (min)	$D_{sv} \times 10^{-9}$ (m ² /s)
30	0.3	58.82	0.6	77.51	0.72	90.9	0.86
	0.6	55	0.65	72	1.05	73	0.91
	1	48	1	69.44	1.18	69.44	0.99
	3	96	0.4	69.93	0.7	81.96	0.79
	5	98	0.38	70.92	0.63	95	0.70
	10	100	0.36	142.85	0.51	163.93	0.46
	15	120	0.32	150	0.48	238.09	0.37
40	0.3	55	1.25	62	0.99	83.33	0.91
	0.6	50	1.70	50	1.25	62.11	1.05
	1	47.61	2.07	48.78	1.70	60.60	1.10
	3	95.23	0.44	58.82	0.71	76	0.89
	5	97	0.39	66.66	0.69	85.47	0.74
	10	98	0.37	69	0.49	90.90	0.57
	15	111.11	0.35	72.99	0.45	100	0.44
50	0.3	35.71	1.73	55.55	1.11	58.82	1.07
	0.6	33.33	1.90	47.61	1.29	43.47	1.11
	1	32.25	2.44	37	1.80	38.46	1.26
	3	90.90	0.68	40.60	0.93	74.07	0.92
	5	95.23	0.59	45	0.48	78	0.76
	10	95	0.55	53	0.47	88	0.59
	15	105.26	0.44	64	0.43	83	0.48
60	0.3	26.31	1.82	46.51	1.25	41.66	1.15
	0.6	25.64	2.50	40	1.80	37.03	1.89
	1	22.72	2.95	35.08	1.95	32.25	2.08
	3	83.33	0.76	35.35	1.48	52.63	1.08
	5	89	0.62	38.46	1.13	55.55	0.78
	10	91	0.60	45.45	0.58	58.82	0.61
	15	103.09	0.46	52.63	0.65	76.92	0.51

composite gel swell less than the gel formed at the critical point, then it takes less time to dry causing larger D_d values. In other words, stiff gel dries faster compared to the loose gel, which is formed at the critical point.

5. Conclusion

This study has demonstrated that the fluorescence method can be used to monitor the drying and swelling behaviours of PAAm-MWNT composite gel prepared with various MWNT content and measured at different temperatures. A moving boundary model combined with Stern-Volmer kinetics was used to measure the desorption coefficient, D_d , for drying processes. It was observed that high MWNT content composites dry much faster, as the result of having larger D_d coefficients for all measurements. A similar fluorescence method was employed to measure the swelling time constants, τ_s , and cooperative diffusion coefficients, D_s , for composite samples prepared with various MWNT contents. The Li-Tanaka Model combined with Stern-Volmer kinetics was used to measure the cooperative diffusion coefficients for the swelling process at various temperatures. The results were interpreted in terms of the swelling time constants; τ_s (decreased) and the cooperative diffusion coefficient D_s (increased) vs. wt% MWNT content. It was observed that high MWNT content composites swell much slower producing smaller D_s coefficients for all measurements at a given temperature.

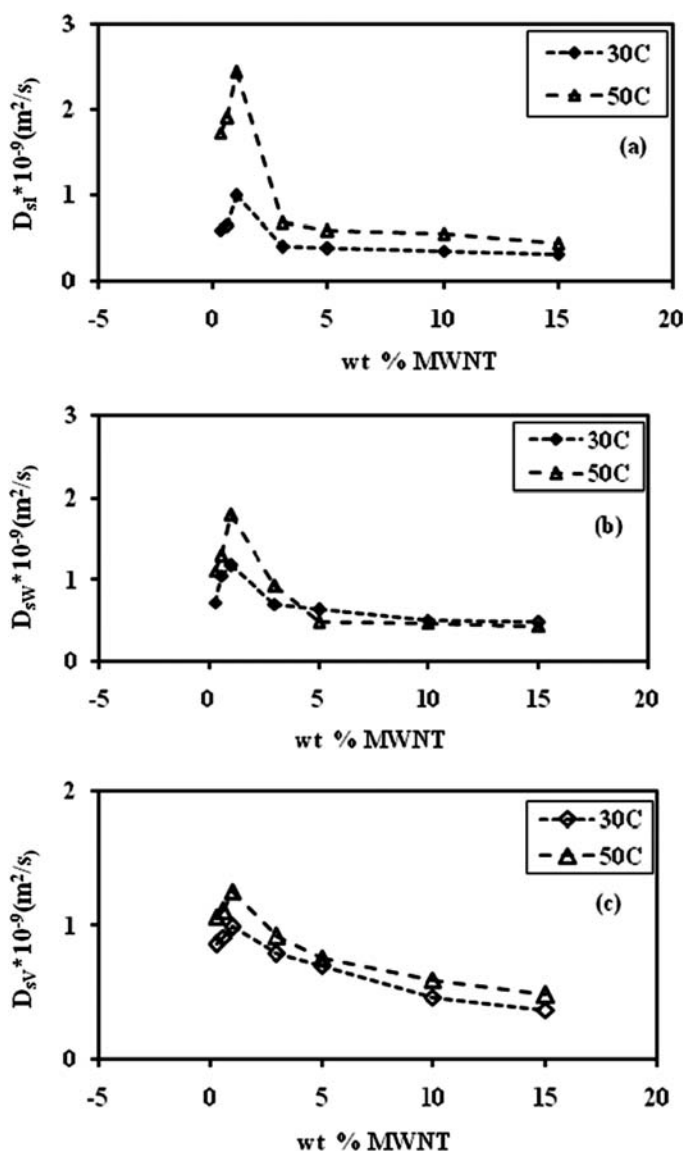


Figure 7. Cooperative diffusion coefficient, D_s , vs. MWNT content measured by (a) fluorescence, (b) gravimetric and (c) volumetric methods at 30 and 50 °C, respectively.

Acknowledgement

Experiments were done in the Spectroscopy Laboratory in the Department of Physics Engineering of İstanbul Technical University. We would like to thank Turkish Academy of Science (TUBA) for the partial support.

References

- [1] Coleman JN, Khan U, Blau WJ, Gun'ko YK. Small but strong: A review of the mechanical properties of carbon nanotube- polymer composites. *Carbon*. 2006;44:1624–52.

- [2] Li H, Wang DQ, Chen HL, Liu BL, Gao LZ. A novel gelatin – carbon nanotubes hybrid hydrogel. *Macromolecular Bioscience*. 2003;3:720–4.
- [3] Li H, Wang DQ, Chen HL, Liu BL, Gao LZ. Synthesis of a novel gelatin – carbon nanotubes hybrid hydrogel. *Colloids and Surfaces B*. 2003;33:85–8.
- [4] Andrews R, Weisenberger MC. Carbon nanotube polymer composites. *Current Opinion in Solid State & Materials Science*. 2004;8:31–7.
- [5] Tong X, Zheng J, Lu Y, Zhang Z, Cheng H. Swelling and mechanical behaviors of carbon nanotube/poly(vinyl alcohol) hybrid hydrogels. *Materials Letters*. 2007;61:1704–6.
- [6] Barone PW, Yoon H, Garcia RO, Zhang J, Ahn JH, Kim JH, Strano MS. Modulation of single walled carbon nanotube photoluminescence by hydrogel swelling. *ACS Nano*. 2009;3(12):3869–77.
- [7] Miyako E, Nagata H, Hirano K, Hirotsu T. Photodynamic thermoresponsive nanocarbon – polymer gel hybrids. *Small (Weinheim an der Bergstrasse, Germany)*. 2008;4(10):1711–5.
- [8] Luo YL, Zhang CH, Chen YS, Yang W. Preparation and characterisation of polyacrylamide/MWNTs nanohybrid hydrogels with microporous structures. *Materials Research Innovations*. 2009;13(1):18–27.
- [9] Satarkar NS, Johnson D, Marrs B, Andrews R, Poh C, Gharaibeh B, Saito K, Anderson KW, Hilt JZ. Hydrogel – MWNT nanocomposites: Synthesis, characterization, and heating with radiofrequency fields. *Journal of Applied Polymer Science*. 2010;117:1813–9.
- [10] Liu H, Liu M, Zhang L, Ma L, Chen J, Wang Y. Dual – stimuli sensitive composites based on multiwalled carbon nanotubes and poly(N, N-diethylacrylamide-co-acrylic acid) hydrogels. *Reactive & Functional Polymers*. 2010;70:294–300.
- [11] Pa PM, Siddiqui NA, Marom G, Kim JK. Dispersion and functionalization of carbon nanotubes for polymer based nanocomposites: A review. *Composites Part A*. 2010;41:1345–67.
- [12] Meena R, Prasad K, Mehta G, Siddhanta AK. Synthesis of the copolymer hydrogel K-carrageenan-graft-PAAm: Evaluation of its absorbent and adhesive properties. *Journal of Applied Polymer Science*. 2006;102:5144–53.
- [13] Bastide J, Duoplessix S, Picot C, Candau SJ. Small angle neutron scattering and light spectroscopy investigation of polystyrene gels under osmotic deswelling. *Macromolecules*. 1984;17(1):83–93.
- [14] Peters A, Candau SJ. Kinetics of swelling of spherical and cylindrical gels. *Macromolecules*. 1988;21:2278–82.
- [15] Zirinyi M, Rosta J, Horkay F. Studies on the swelling and shrinking kinetics of chemically cross-linked disc-shaped poly(vinylacetate) gels. *Macromolecules*. 1993;26:3097–102.
- [16] Akın Evingür G, Pekcan Ö. Drying of polyacrylamide composite gels formed with various kappa – carrageenan content. *Journal of Fluorescence*. 2011;21:1531–7.
- [17] Akın Evingür G, Pekcan Ö. Kinetics models for the dynamical behaviors of PAAm-κ-carrageenan composite gels. Submitted to *Journal of Bioactive and Compatible Polymers*, November 2011.
- [18] Erdogan M, Pekcan Ö. Drying of heterogels swollen in organic vapor. *Composite Interfaces*. 2003;10(6):547–66.
- [19] Erdogan M, Pekcan Ö. Fast transient fluorescence method for measuring swelling and drying activation energies of a polystyrene gel. *Polymer*. 2004;45:2551–8.
- [20] Pekcan Ö, Kara S. Photon transmission technique for monitoring formation and swelling of acrylamide gels. *Polymer – Plastics Technology and Engineering*. 2001;41(3):573–88.
- [21] Pekcan Ö, Kara S. Photon transmission technique for monitoring swelling of acrylamide gels formed with various crosslinker contents. *Polymer*. 2001;42:10045–53.
- [22] Aktaş DK, Akın Evingür G, Pekcan Ö. Study on swelling of hydrogels(PAAm) at various temperatures by using fluorescence technique. *Journal of Materials Science*. 2007;42:8481–8.
- [23] Aktaş DK, Akın Evingür G, Pekcan Ö. A fluorescence study on swelling of hydrogels(PAAm) at various crosslinker contents. *Advances in Polymer Technology*. 2009;28(4):215–9.
- [24] Akın Evingür G, Pekcan Ö. Temperature effect on the swelling of PAAm-κ-carregeenan composites. *Journal of Applied Polymer Science*. 2012;123:1746–54.
- [25] Birks JB. *Photophysics of aromatic molecules*. New York, NY: Wiley; 1971.
- [26] Crank J. *The mathematics of diffusion*. Oxford: Clarendon Press; 1975.
- [27] Li Y, Tanaka T. Kinetics of swelling and shrinking of gels. *Journal of Chemical Physics*. 1990;92:1365–71.
- [28] Aktaş DK, Akın Evingür G, Pekcan Ö. Critical exponents of gelation and conductivity in Polyacrylamide gels doped by multiwalled carbon nanotubes. *Composite Interfaces*. 2010;17:301–18.

- [29] Yılmaz Y, Uysal N, Gelir A, Guney O, Aktaş DK, Gogebakan S, Oner A. Elucidation of multiple-point interactions of pyranine fluoroprobe during the gelation. *Spectrochimica Acta, Part A: Molecular and Biomolecular Spectroscopy*. 2009;72:332–8.
- [30] Kaya D, Pekcan Ö, Yılmaz Y. Direct test of the critical exponents at the sol-gel transition. *Physical Review E*. 2004;69(1–10):16117.